Earthquakes and Structures, *Vol. 11, No. 6 (2016) 1101-1121*
DOI: http://dx.doi.org/10.12989/eas.2016.11.6.1101

Semi-active storey isolation system employing MRE isolator with parameter identification based on NSGA-II with DCD

Xiaoyu Gu, Yang Yu, Jianchun Li**, Yancheng Li* and Mehrisadat Makki Alamdari

Centre for Built Infrastructure Research, Faculty of Engineering and IT, University of Technology, Sydney, Australia

(Received March 10, 2016, Revised June 19, 2016, Accepted July 17, 2016)

Abstract. Base isolation, one of the popular seismic protection approaches proven to be effective in practical applications, has been widely applied worldwide during the past few decades. As the techniques mature, it has been recognised that, the biggest issue faced in base isolation technique is the challenge of great base displacement demand, which leads to the potential of overturning of the structure, instability and permanent damage of the isolators. Meanwhile, drain, ventilation and regular maintenance at the base isolation level are quite difficult and rather time- and fund- consuming, especially in the highly populated areas. To address these challenges, a number of efforts have been dedicated to propose new isolation systems, including segmental building, additional storey isolation (ASI) and mid-storey isolation system, etc. However, such techniques have their own flaws, among which whipping effect is the most obvious one. Moreover, due to their inherent passive nature, all these techniques, including traditional base isolation system, show incapability to cope with the unpredictable and diverse nature of earthquakes. The solution for the aforementioned challenge is to develop an innovative vibration isolation system to realise variable structural stiffness to maximise the adaptability and controllability of the system.

Recently, advances on the development of an adaptive magneto-rheological elastomer (MRE) vibration isolator has enlightened the development of adaptive base isolation systems due to its ability to alter stiffness by changing applied electrical current. In this study, an innovative semi-active storey isolation system inserting such novel MRE isolators between each floor is proposed. The stiffness of each level in the proposed isolation system can thus be changed according to characteristics of the MRE isolators. Non-dominated sorting genetic algorithm type II (NSGA-II) with dynamic crowding distance (DCD) is utilised for the optimisation of the parameters at isolation level in the system. Extensive comparative simulation studies have been conducted using 5-storey benchmark model to evaluate the performance of the proposed isolation system under different earthquake excitations. Simulation results compare the seismic responses of bare building, building with passive controlled MRE base isolation system, building with passive-controlled MRE storey isolation system and building with optimised storey isolation system.

Keywords: storey isolation system; magneto-rheological elastomer; five-storey building model; genetic algorithm; optimisation

---

*Corresponding author, E-mail: Yancheng.li@uts.edu.au
**Corresponding author, E-mail: Jianchun.Li@uts.edu.au

http://www.techno-press.com/journals/eas&subpage=7 ISSN: 2092-7614 (Print), 2092-7622 (Online)

1. Introduction

Earthquake, the third killer to capture human lives in addition to war and pestilence, has caused great loss to the human society, not only by claiming countless lives, but also swallowing enormous material prosperity and social civilization (Kelly 1986). Despite rapid development of technology, the problems and great danger ensued from earthquakes has not been resolved or even effectively reduced, especially in undeveloped seismic countries, mainly due to the great density of population and lack of seismic protection measures in structural design (Gilmore 2012, Tornello and Sarrazin 2012). As a matter of fact, if not properly designed, a low- to mid-rise building can behave like an amplifier to the seismic energy since the fundamental frequencies of conventional buildings usually drop in the range of dominant earthquake frequencies, which results in vibration resonance (Jangid and Kelly 2001, Wang *et al*. 2016). As a consequence, the acceleration experienced at each level increases with the height of structure, resulting in hazard to structural and non-structural elements of the building.

For over one hundred years, great efforts have been made by engineers and architects to reduce the response of the structure due to ground movement, among which base isolation system is a maturing technology proven to be effective over the decades and becomes the most widely applied seismic protection mechanism (Jangid and Datta 1995). In short, the working principle of base isolation system is to decouple the superstructure from the ground motion by softening the connection layer between the building and ground (Johnson *et al*. 1998). Such soft layer endows the base level with a much smaller stiffness compared with the fixed base building and thus effectively shifts the fundamental frequency of the structure from earthquake dominant frequency to avoid resonance (Kelly 1981).

However, although proven to be effective in numerous practical applications worldwide (Kelly 1993), base isolation technique has its own flaws, among which large base displacement is the most concerned issue (building code provisions for seismic base isolation UBC 1991). During earthquake excitation, if the base isolation system is designed properly, the superstructure decoupled from ground motion behaves a rigid body motion, which ensures great reduction of inter-storey drift but leads to relatively enormous displacement across the base isolation level (Pan and Wei 1998). Therefore, the foundation level of conventional base-isolated structure is demanded to provide adequate lateral flexibility to satisfy the massive base displacement requirement of the base isolation system, which is more time-consuming and less economical efficient in terms of implementation and construction (Jangid and Datta 1995). Meanwhile, even the structural element can meet base displacement prerequisite, large deformation of the base isolators also lead to buckling phenomenon and thus raise issues of instability, etc. (Forcellini *et al*. 2013) Secondly, the natural frequencies of the structure are inversely proportional to its flexibility, which increases with the height and slenderness of the building. Hence, the capability of shifting structural frequency of the base isolation system reduces when structure becomes more flexible and slender, which restrains the range of applicable structure to only low- to mid-rise buildings (Skinner *et al*. 1993).

The motivation to mitigate problems above has driven researchers to come up with various resolutions and alternations of the conventional base isolation systems. In 1993, Pan *et al*. proposed a concept of segmental buildings to divide the superstructure into several segments and each of two segments are interconnected by additional isolation systems. Numerical studies of the proposed concept are conducted and it is proven that the segmental building can effectively reduce base displacement but the displacements of higher levels are amplified to some extent when compared to base-isolated structure (Pan *et al*. 1995). Additional storey isolation (ASI) strategy was proposed by Chey *et al*. (2013) to behave as a tuned mass damper (TMD) system for seismic retrofit of existing building. Isolation level is inserted between the added level and original building so as to dissipate seismic energy via isolation level to reduce the seismic force experienced by the structure. Such approach achieves good seismic retrofitting performance but the large displacement in isolation level becomes a major hidden danger. Mid-storey isolation is also an alternative strategy gaining popularity to replace base isolation system. Many residential-commercial buildings with mid-storey isolation system have been put into use around the world, especially in China, Korea and Japan (Zhong *et al*. 2004, Wang *et al*. 2012, Torunbalci and Ozpalanlar 2008, Sueoka *et al*. 2004, Kawamura *et al*. 2000). At the moment, the mid-storey isolation system is mainly equipped in the high-rise buildings where overturning is one of the significant concerns with the isolation system (Chey *et al*. 2009). However, despite high popularity, the mid-storey isolation system is still a weak link in the building.

The authors (Gu *et al*. 2014) have proposed a novel semi-active multi-storey isolation system, which can be recognised as a combination and extension of segmental building and mid-storey isolation system. The bearing employed in this system is an innovative adaptive magneto-rheological elastomer (MRE) isolator designed and manufactured by Li *et al*. (2013b). The MRE isolator follows the classical laminated rubber bearing design, but innovatively replaced the traditional rubber with the smart material MRE whose shear modulus can be significantly changed by altering applied magnetic flux. Therefore, the storey isolation system acquires changeable lateral stiffness, which allows it to change the structural properties and thus adapt to various disturbances. By interpolating the isolation system into different levels of the structure, the storey isolation system distributes the flexibility along the entire building which was concentrated at base level in base isolation case. During earthquake excitation, all storey isolation levels collaboratively absorb and dissipate energy instead of only by one isolation system. As a result, the displacement demand at each isolation level will be much smaller than that of a solely base-isolated structure. Moreover, it is revealed by literatures (Ryan *et al*. 2010, Jin *et al*. 2012, Murakami *et al*. 2000) that in the mid-storey isolations system, the building has different seismic protection performance in the structure upper and lower than the isolation level. In contrast, the storey isolation is capable of reducing seismic response to the greatest degree in every storey. Another common problem often encountered by the mid-storey isolation or additional storey isolation system is whipping effect, which will significantly amplify the velocity and displacement of the upper structure if resonance occurs. Attribute to the adaptability of the proposed storey isolation system provided by the smart MRE isolators, the structural component stiffness and thus frequency can be simply adjusted according to the excitation property, which allows the system great adaptability and controllability.

In this paper, the design and modelling of the MRE isolator will be firstly briefed, followed by a detailed elaboration of the concept and design of the storey isolation system. An improved non-dominated sorting genetic algorithm type II (NSGA-II) is adopted to identify the optimised parameters of each storey isolation level. The novelty of the methodology lies in the introduction of dynamic crowding distance (DCD) into the algorithm as an evaluative index to keep good diversity among the solution. Four benchmark earthquake records are used in this study, which are El-Centro 1940, Kobe 1995, Hachinohe 1968 and Northridge 1994. Comparative numerical studies are conducted using a five-storey benchmark building model to evaluate the seismic protection performance of the fixed-based building, base-isolated building, passive storey-isolated building and optimised storey-isolated building. Simulation results indicate that the seismic resistance performance of the building with optimal storey isolation system is significantly

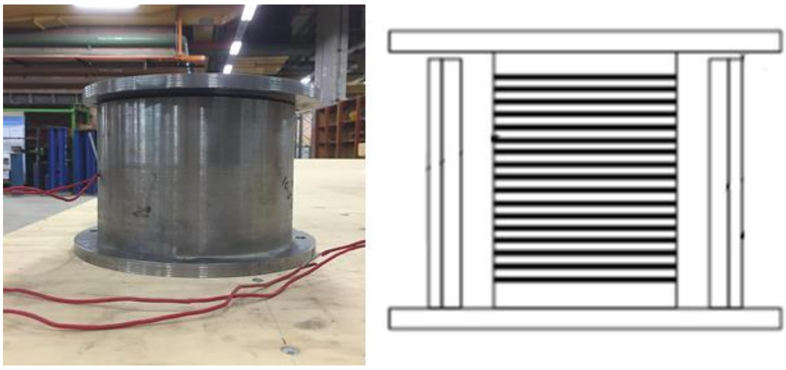

Fig. 1 Photo and schematic diagram of MRE isolator

superior to the bare frame, building with passive base isolation system and building with passive storey isolation system when subjected to different types of earthquakes.

2. Magnetorheological Elastomer (MRE) isolator

2.1 Brief introduction on MRE isolator

Li *et al*. (2012, 2013a) have proposed and fabricated an adaptive magnetorheological elastomer (MRE) isolator and comprehensive characterization of the isolator has been conducted. In this design, a soft MRE material, a kind of smart material, is employed as the core material, which consists of silicon rubber as the material matrix, carbonyl iron particles as the ferromagnetic particle and silicon oil as the additive to assist iron particles to be dispersed in matrix evenly. When applied magnetic field, the array of the carbonyl iron particles will be changed so as to vary the shear modulus of the material, which is known as MR effect. The material's properties, especially for MR effect, have been tested and significant MR effect has been observed regards to this new soft MRE material.

The MRE base isolator follows the design of traditional laminated rubber bearing (LRB) but substitutes the conventional rubber with MRE material. The photo and schematic diagram are shown in Fig. 1. As shown in Fig. 1, thin plates of MRE sheet and steel plates are arranged alternately to form the core of a sandwich structure. Altogether there are 25 layers of MRE and 26 layers of steel plates vulcanized and bonded side by side. The thickness of both sheet metals is 1 mm. The principle behind such design is that the existence of steel plates is to provide high vertical loading capacity and prevent the MRE layer from bulging while the MRE material can provide flexibility and variable stiffness in horizontal direction. Two steel plates are tabbed to the top and bottom of the core structure to close the device and make it easy to implement the device to any structure. An electromagnetic solenoid is placed around the laminated structure so as to energise the MRE layers with uniformed magnetic field. Finally, a steel yoke is to house the coil and laminated core inside and provide necessary support if the whole structure fails. There is a gap of 2 mm between the top plate and steel yoke to avoid touching and consequential friction. The inner diameter of coils is 150 mm while the diameter of the laminated structure is 120 mm, which allows a maximum 15 mm deformation of the isolator under vibration excitation. The design of the

MRE isolator, on the other hand, restricts the displacement of the isolation layer in practical appliance since although the device will not necessarily diminish after reaching the maximum deformation, the bumping of the core and coil yoke will result in bad influence on vibration mitigation performance.

2.2 Modeling of MRE isolator

As mentioned in last section, a series of comprehensive tests have been executed for the characterisation of the MRE isolator. Based on the experimental data, several models of the device have been proposed by Yu *et al*. (2015, 2016). Effective stiffness of the isolator can be indirectly measured knowing the deformation and corresponding shear force generated by the isolator under different circumstance. The experimental setup for the shake table testing is shown below in Fig. 2. The shear force can be recorded by the load cell while displacement of the shake table represents the deformation of the isolator. During the tests, the isolator was subjected to different magnetic flux density generated by current of 0A, 1A, 2A and 3A. Meanwhile, the motions of the shake table are sinusoidal waves with amplitude of 2 mm, 4 mm and 8 mm and each amplitude of displacement corresponds to frequencies of 1 Hz, 2 Hz and 4 Hz. The effective stiffness and equivalent damping coefficients under different conditions are listed in Table 1 and Table 2.

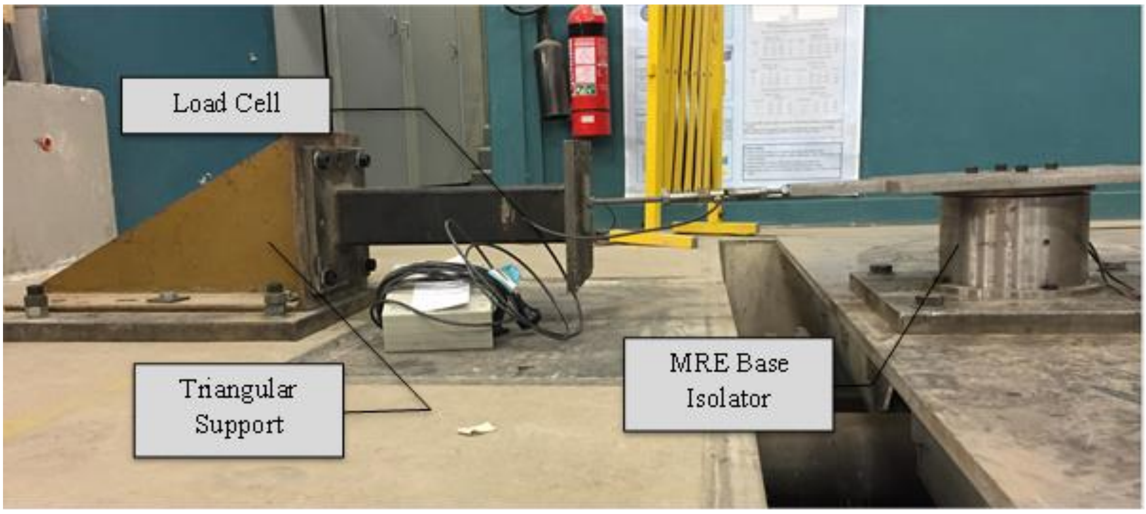

Fig. 2 Photo of testing setup

Table 1 Effective stiffness values of device under different excitation conditions

Effective stiffness (kN/m)	2 mm			4 mm			8 mm		
	1 Hz	2 Hz	4 Hz	1 Hz	2 Hz	4 Hz	1 Hz	2 Hz	4 Hz
0A	4.96	5.80	6.88	4.69	5.33	6.43	4.62	5.24	6.23
1A	27.13	27.52	27.75	20.72	20.87	21.07	17.72	17.81	18.12
2A	52.22	50.64	50.47	38.15	37.53	37.25	31.44	31.15	31.30
3A	66.13	65.02	65.26	48.74	47.88	47.72	39.31	39.29	39.30

Table 2 Equivalent damping of device under different excitation conditions

Equivalent damping(kN·s/m)	2 mm			4 mm			8 mm		
	1 Hz	2 Hz	4 Hz	1 Hz	2 Hz	4 Hz	1 Hz	2 Hz	4 Hz
0A	0.35	0.22	0.14	0.33	0.21	0.14	0.30	0.19	0.13
1A	2.07	1.09	0.61	1.50	0.81	0.46	1.15	0.63	0.37
2A	3.62	1.87	1.01	2.50	1.31	0.73	1.88	1.00	0.56
3A	4.23	2.19	1.19	2.94	1.53	0.85	2.24	1.18	0.66

Table 3 Parameter values

Parameter	Value
k_m^1 (kN/m·I)	15.41
k_m^0 (kN/m)	6.544
c_m^1 (kN·s/m·I)	0.5643
c_m^0 (kN·s/m)	0.3254

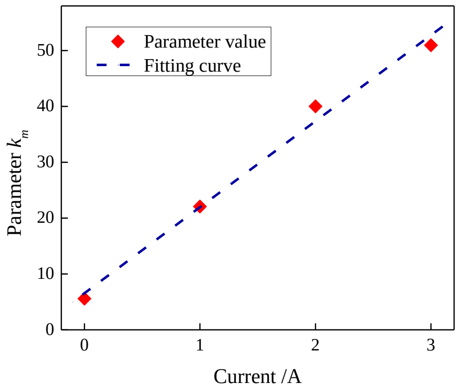

(a) k_m vs current

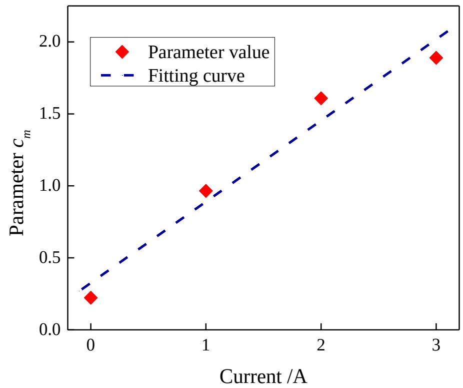

(b) c_m vs current

Fig. 3 Relationships between device properties and applied currents

Next, the stiffness and damping properties of MRE isolator are grouped and averaged according to different applied current levels. Fig. 3 gives the relationship between averaged properties and current level. Curve fitting of the two graphs clearly illustrates that there is a linear relationship between the average effective stiffness km and applied current as well as the average equivalent damping coefficient cm and applied current. It is obvious that the first order polynomial function can be used to set up current-dependent models. The equations are shown as following

$$k_m(I) = k_m^1 \times I + k_m^0 \tag{1}$$

$$c_m(I) = c_m^1 \times I + c_m^0 \tag{2}$$

Then, least square (LS) method is employed to identify the model parameters based on root mean square (RMS) errors between actual mean values and predictions from the model. The results of model identification are given in Table 3.

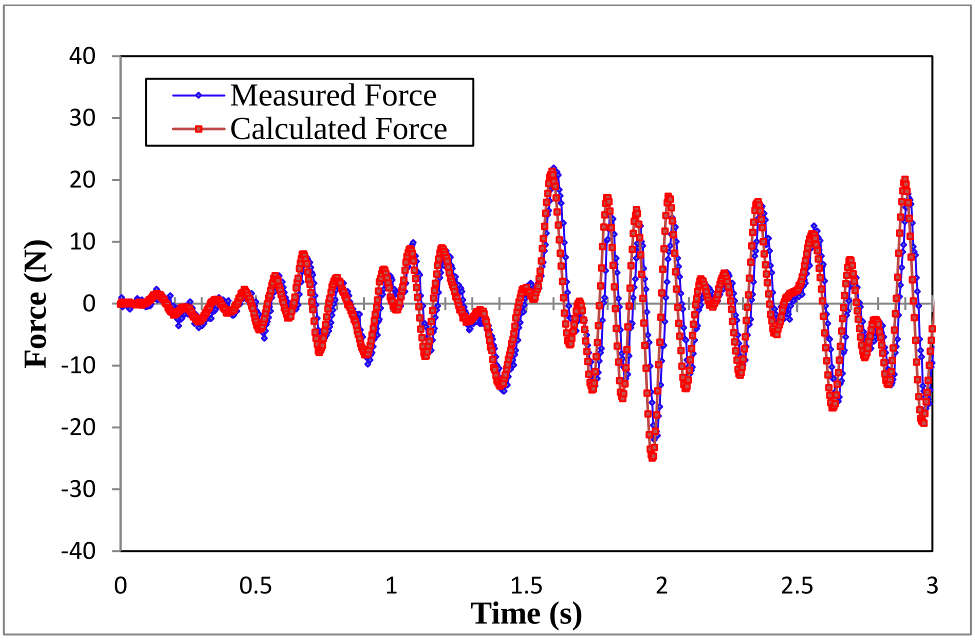

Fig. 4 Comparison of experimental and predicted forces based on random test data (current=0A)

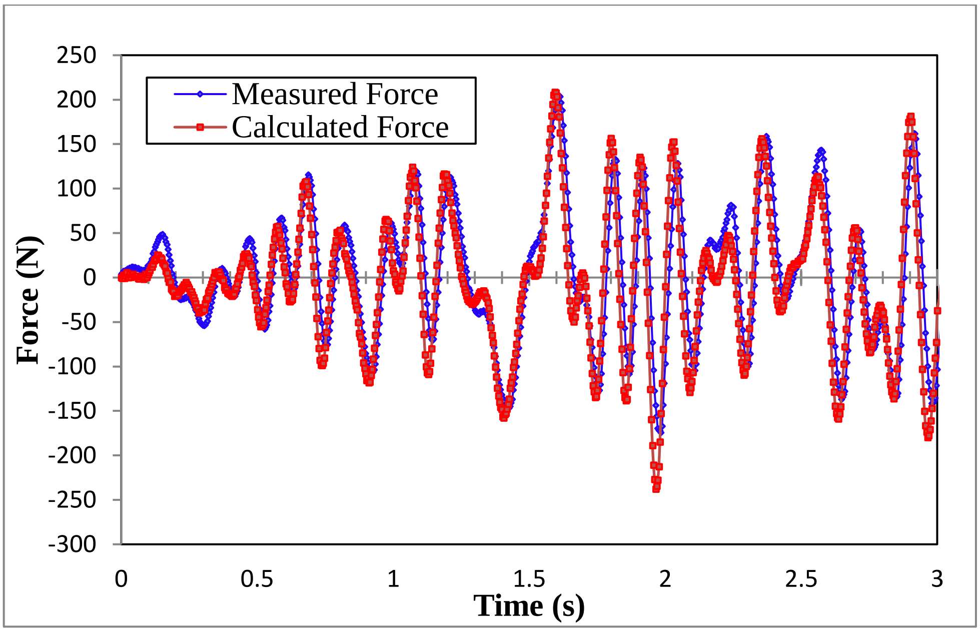

Fig. 5 Comparison of experimental and predicted forces based on random test data (current=3A)

To validate the reliability of the proposed model of MRE isolator, a series of dynamic tests are conducted based on the random displacement excitation. The random displacement signal is generated with a maximum amplitude of 5 mm and excitation frequency between 1 and 20 Hz.

Two cases with 0 current input and maximum current input (3A) are taken into consideration for the comparison of the force generated by isolator under random current input and the force predicted by the proposed model. The sampling time and frequency for all dynamic tests is set as 2 s and 256 Hz, respectively. Fig. 4 and Fig. 5 illustrate the force measured by the load cell and predicted results from the model. It can be clearly observed that, in both cases, satisfactory agreement of predicted force can be provided by the model. In a word, the fitting results verify the feasibility and reliability of this model for its application in the vibration control of building structures using MRE base isolator.

3. Storey isolation model

The storey isolation system proposed in this paper is a novel isolation approach to incorporate the isolation system not only under the superstructure, but also in between adjacent floors. The schematic diagram of the storey isolation system is shown in Fig. 6. In this design, the isolation system is able to distribute flexibility alongside the height of the building so as to significantly reduce the displacement demand and burden on the base isolation level. Meanwhile, the storey isolation system will not sacrifice but in contrast possibility enhance the effectiveness of seismic protection in that it can interrupt the seismic energy flux level by level so as to decouple every single level from the structure beneath it. The MRE isolators are installed into the storey isolation system and its adaptable stiffness characteristic allows changeable and controllable stiffness at each degree of freedom (DOF) of the entire building. MRE isolator’s dynamic features can be tuned by adjusting input current to cope with both earthquake excitations and small external interference during normal situations. Meanwhile, the MRE isolators are able to perform adaptive tuning based on instant measurement of the civil structure, whose characters may be changed from time to time or due to damage. Such trait ensures better after-shock resilience of the structure and better adaptability to damages occurred in the structure.

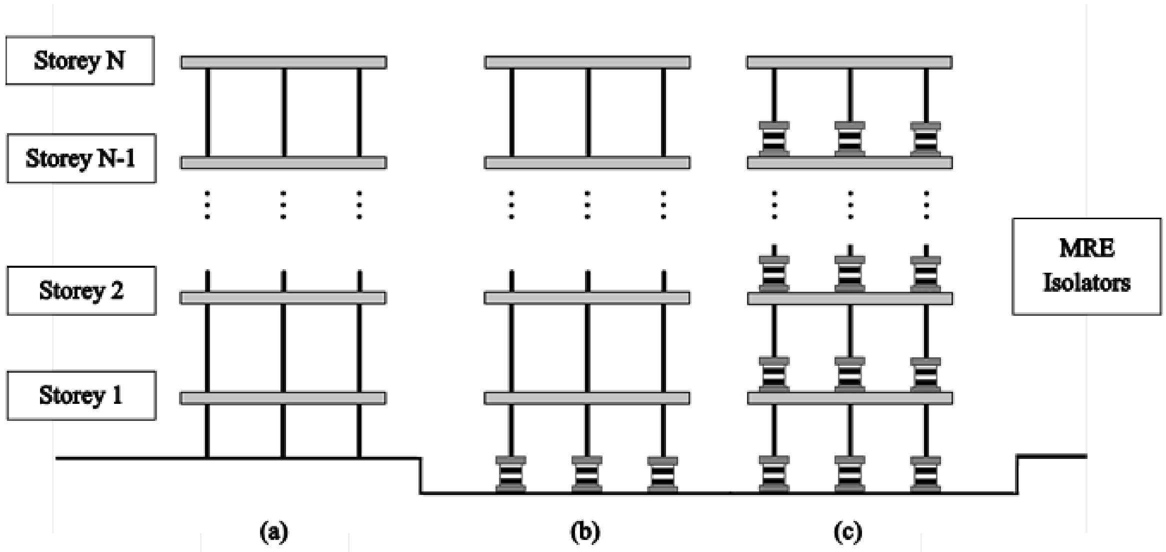

Fig. 6 Schematics of (a) fixed base building, (b) base-isolated building and (c) storey-isolated building

Assume a civil structure with N levels, since only the movement along the direction of ground motion is of interest, the building can be simplified as an N-DOF lumped mass model. The mass, stiffness and damping coefficient at the ith level of the original building are mi, ki and ci. In the case of storey isolation system, the MRE isolators at each floor are in series connection with the original structural elements. Therefore, equivalent stiffness $\mathrm{k_{ie}}$ and damping coefficient c_{ie} of the ith level can be written as

$$k_{ie} = \frac{k_i \cdot k_m(I_i)}{k_i + k_m(I_i)} \tag{3}$$

$$c_{ie} = \frac{c_i \cdot c_m(I_i)}{c_i + c_m(I_i)} \tag{4}$$

where I_i is the current applied to the isolators at the ith level. The sketches of the fixed base building, base-isolated building and storey-isolated building are shown in Fig. 7. The stiffness and damping matrices of the storey isolation system model are written in Eqs. (5) and (6). As can be seen from the matrices, the structural parameters of the storey isolation system can be simply controlled by altering the applied current to the isolators at each level.

$$K = \begin{bmatrix} k_{1e}+k_{2e} & -k_{2e} & 0 & \cdots & 0 & 0 & 0 \\ -k_{2e} & k_{2e}+k_{3e} & -k_{3e} & \cdots & 0 & 0 & 0 \\ \vdots & \vdots & \vdots & \vdots & \vdots & \vdots & \vdots \\ 0 & 0 & 0 & \cdots & -k_{(n-1)e} & k_{(n-1)e}+k_{ne} & -k_{ne} \\ 0 & 0 & 0 & \cdots & 0 & -k_{ne} & k_{ne} \end{bmatrix} \tag{5}$$

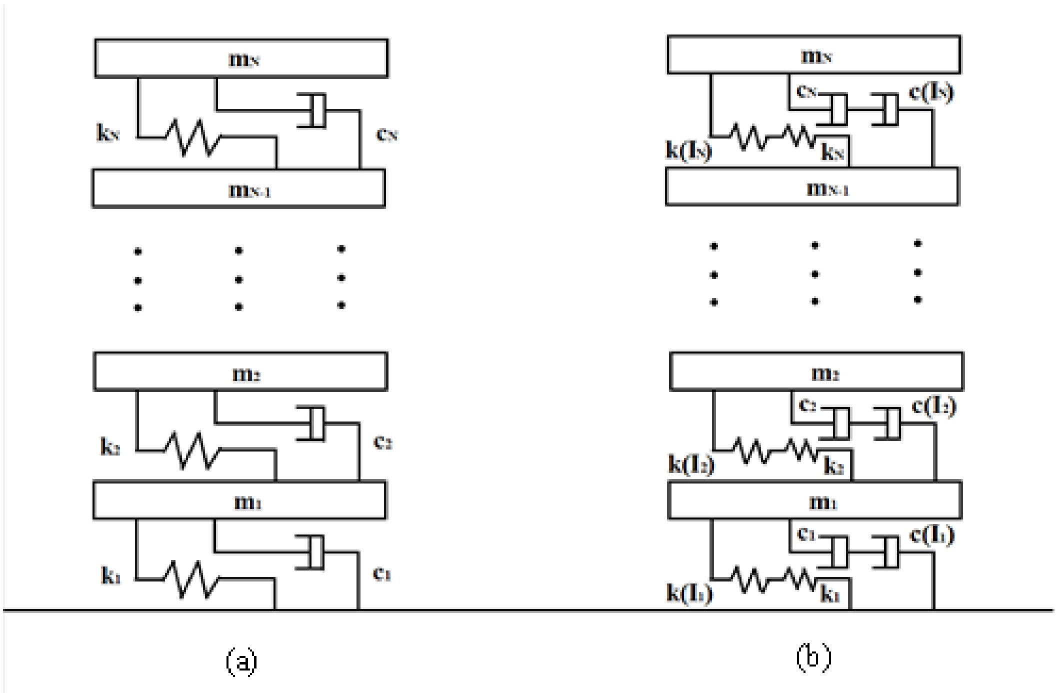

Fig. 7 Sketches of the (a) fixed base building and (b) storey-isolated building

$$C=\begin{bmatrix} c_{1e}+c_{2e} & -c_{2e} & 0 & \cdots & 0 & 0 & 0 \\ -c_{2e} & c_{2e}+c_{3e} & -c_{3e} & \cdots & 0 & 0 & 0 \\ \vdots & \vdots & \vdots & \vdots & \vdots & \vdots & \vdots \\ 0 & 0 & 0 & \cdots & -c_{(n-1)e} & c_{(n-1)e}+c_{ne} & -c_{ne} \\ 0 & 0 & 0 & \cdots & 0 & -c_{ne} & c_{ne} \end{bmatrix} \tag{6}$$

4. Optimal parameter identification

4.1 Optimisation problem statement

To find out the optimal current values applied to the proposed system is of great significance in generating the guideline for system design, which is also considered as solving the multi-objective optimisation problem. The primary objective of model parameter optimisation is to set up the suitable fitness functions. In this study, four important indices, peak floor acceleration, peak inter-storey drift, root mean squared (RMS) floor acceleration and RMS inter-storey drift, are selected to construct the fitness functions. Mathematical expressions of those functions are given as following:

(1) Peak floor acceleration

$$PFA=\max_{k,t}\{|\ddot{x}_k(t)|\} \tag{7}$$

where k denotes the storey number and $\ddot{x}$ denotes the floor acceleration.

(2) Peak inter-storey drift

$$PISD=\max_{k,t}\{|\bar{x}_k(t)|\} \tag{8}$$

where $\bar{x}$ denotes the inter-storey drift.

(3) Root mean squared (RMS) floor acceleration

$$RMS_{FA}=\sqrt{\frac{1}{T}\sum\Delta t\cdot\ddot{x}_k^2(t)} \tag{9}$$

where T denotes the sampling period and Δt denotes the sampling interval.

(4) RMS inter-storey drift

$$RMS_{ISD}=\sqrt{\frac{1}{T}\sum\Delta t\cdot\bar{x}_k^2(t)} \tag{10}$$

The fitness functions are defined as the maximal values of indices above under four benchmark earthquake excitations of EI-Centro, Kobe, Hachinohe and Northridge. The minimization optimization problem for optimal applied currents can be written as below:

$$\begin{aligned} &\text{minimize } obj_1=\max\{PFA\}_{\substack{EI-Centro\\Kobe\\Northridge\\Hachinohe}},\ obj_2=\max\{PISD\}_{\substack{EI-Centro\\Kobe\\Northridge\\Hachinohe}}, \\ &\qquad obj_3=\max\{RMS_{FA}\}_{\substack{EI-Centro\\Kobe\\Northridge\\Hachinohe}},\ obj_4=\max\{RMS_{ISD}\}_{\substack{EI-Centro\\Kobe\\Northridge\\Hachinohe}} \\ &s.t.\quad 0\le I_i\le I_{\max},\ \ i=1,2,...,k \end{aligned} \tag{11}$$

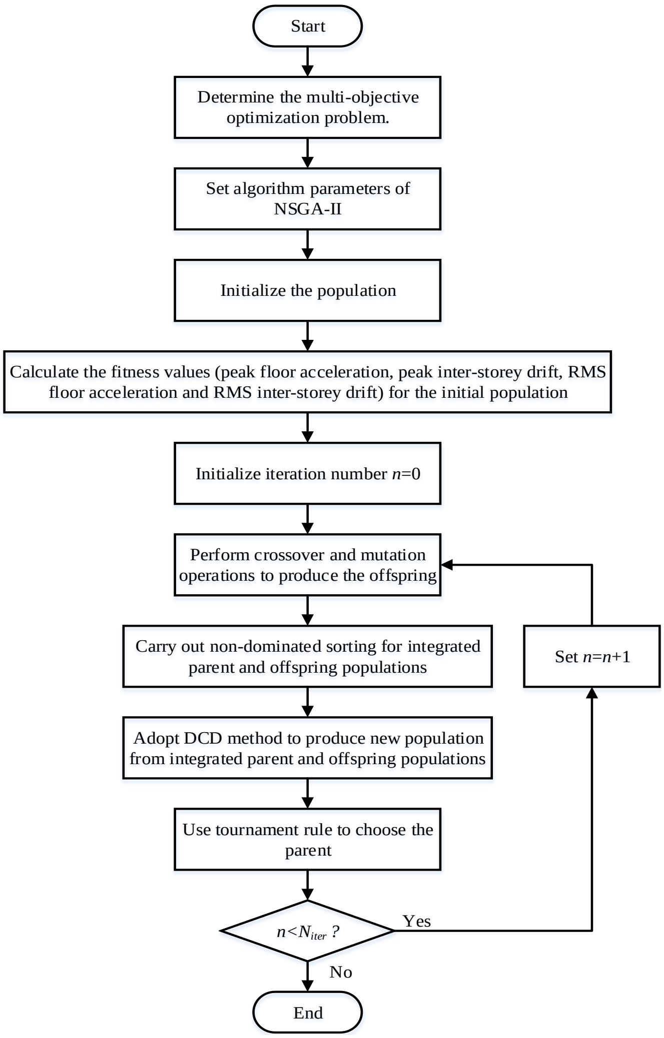

Fig. 8 Flow chart of NSGA-II with DCD to calculate the optimal applied currents

where I_i denotes the current values applied to the MRE base isolator at ith level and Imax dentoes the extreme value of applied current to the device. Imax is set as 5A to maximise the range of adjustability within the capability limit of MRE isolator.

4.2 Parameter identification based on NSGA-II with DCD

In this study, an improved non-dominated sorting genetic algorithm type II (NSGA-II) method is utilised to solve the multi-objective optimization problem. Dynamic crowding distance (DCD) is introduced into the standard NSGA-II as a novel evaluation index to keep good diversity among the solutions. The detailed procedure of NSGA-II with DCD to identify the optimal parameter of the storey isolation system is concluded as the following steps:

1) Determine the multi-objective problem. In this work, the fitness functions are obj_1, obj_2,

obj_3 and obj_4. The parameters to be identified are current levels applied to each MRE base isolator.

2) Set the parameter values of NSGA-II with DCD. Here, the population number is 20, crossover probability is 0.9, mutation probability is 0.15 and maximum iteration number is 100.

3) Initialize the population.

4) Calculate the fitness values.

5) Initialize the iteration number n=0.

6) Carry out the crossover and mutation operations for the individual group.

7) Systematize the population based on every fitness value in an increasing order.

8) Compute the dynamic crowding distances among solutions.

9) Select parent using tournament rule: the individual, on the bare population area of the front, is assigned with the higher fitness value.

10) Increase the iteration number and check the stop criterion. If the current iteration arrives at its maximum value, the algorithm is terminated. Or else, repeat Step 2) to Step 9).

The detailed flow chart of implementation of NSGA-II with DCD to optimize the smart storey isolation system is shown in Fig. 8.

5. Simulation

5.1 Five-storey benchmark building

In order to evaluate the performance of the semi-active storey isolation system utilising MRE isolators presented in last section, comprehensive study of numerical simulation is conducted using a five-storey benchmark building model created by Samali *et al*. (1999). The numerical testing compares the seismic responses of fixed-based building, building with passive-off MRE base isolation system, building with passive-on MRE base isolation system, building with passive-on storey isolation system and building with optimised storey isolation system. The five-storey

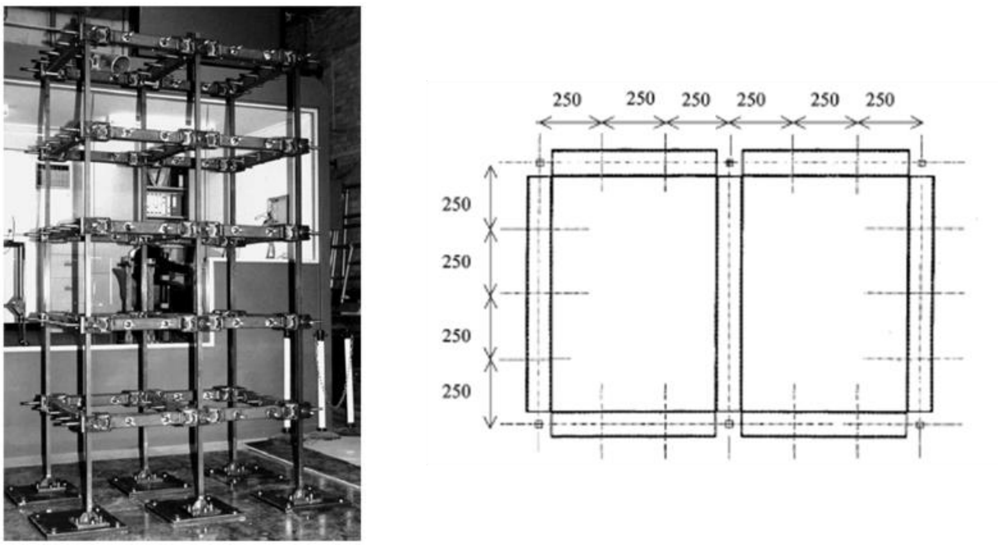

Fig. 9 Photo and typical floor plan of the 5-storey benchmark building model (Wu et al., 2002)

benchmark building model is recognised to be one of the International Association of Structural Control and Monitoring (IASC) experimental building models. The photo and floor plan of the 5-storey building model are shown in Fig. 9 while the structural parameters of the model, including mass, effective stiffness and damping coefficient of each floor, are listed in Table 4.

Table 4 Structural parameters of the 5-storey model

Floor No.	1	2	3	4	5
Mass (kg)	214	207	207	207	207
Stiffness (kN/m)	1146	3124	3156	3156	2978
Damping (kN·s/m)	0.0584	0.1117	0.1128	0.1100	0.1233

Table 3 Optimisation results for current and objective values

Current at each level (A)					***Obj*₁** (g)	***Obj*₂** (mm)	***Obj*₃** (g)	***Obj*₄** (mm)
Level 1	Level 2	Level 3	Level 4	Level 5				
0.061	3.076	2.569	4.253	1.120	158.033	1.159	71.782	0.376
0.061	3.394	2.569	3.902	1.120	160.099	1.137	69.959	0.367
0.000	3.059	2.561	3.729	3.300	142.672	1.231	60.499	0.268
2.544	1.693	1.672	3.740	3.187	41.998	2.834	12.658	0.428
2.534	1.784	1.564	3.740	3.144	43.848	2.745	12.131	0.422
2.308	1.951	1.866	3.112	2.847	37.348	2.522	14.466	0.478
0.438	3.114	2.561	3.759	3.098	105.291	1.268	36.917	0.336
0.000	2.870	2.569	4.198	0.889	140.626	1.416	69.845	0.316
0.965	2.360	1.503	4.595	2.859	63.919	1.550	25.097	0.384
0.715	3.114	3.126	3.759	2.693	84.389	1.432	31.223	0.387
0.132	3.537	2.675	4.241	1.496	151.190	1.374	55.923	0.333
0.480	3.131	2.675	3.982	1.556	95.435	1.327	48.169	0.464
1.216	1.315	1.570	3.516	3.046	53.103	1.542	21.249	0.391
0.612	3.537	2.800	3.765	1.496	85.477	1.425	28.184	0.332
0.000	3.059	2.561	3.729	2.975	143.089	1.214	60.436	0.269
0.529	3.114	2.561	3.729	2.975	99.825	1.285	44.385	0.439
0.536	3.142	2.675	3.982	1.556	97.220	1.386	43.999	0.454
1.434	1.605	1.430	3.835	2.872	48.869	1.679	14.861	0.323
0.000	3.059	2.561	4.058	3.254	142.354	1.244	60.834	0.268
2.039	2.125	1.859	3.112	2.755	43.449	2.232	14.951	0.442
2.231	2.125	1.859	3.112	2.755	39.413	2.066	17.623	0.545
2.231	2.125	1.859	3.112	2.755	39.413	2.066	17.623	0.545
2.231	2.125	1.859	3.112	2.755	39.413	2.066	17.623	0.545
2.231	2.125	1.859	3.112	2.755	39.413	2.066	17.623	0.545
2.231	2.125	1.135	3.278	2.755	51.203	1.938	15.750	0.426
2.231	2.125	2.172	3.112	2.755	47.703	2.240	25.841	0.748
2.977	2.125	1.859	3.112	2.755	43.299	3.308	18.103	0.658

As can be seen in Table 4 and Fig. 9, the self-weight of the 5-storey building model is approximately 1 ton and there are 2 bays W-E and 1 bay N-S. Considering the vertical capacity of individual MRE base isolator under limited displacement (Li *et al*. 2012), 6 MRE isolators were adopted at each isolation level in both base- and storey- isolation systems. In other words, nd = 6 in this case study. Apply NSGA-II with DCD to the 5-storey benchmark building model with adaptive storey isolation system and the optimisation results are displayed in Table 5.

As can be observed from Table 5, there is not much difference in objectives related to inter-storey drift when applied different sets of optimised currents. Therefore, objectives associated with acceleration are of more interest for the decision of optimised current choice. As a result, the set of current marked with grey shadow in Table 5 was chosen to minimise the response of the adaptive storey isolation system under earthquake excitations.

5.1 Simulation results and discussion

Similar to the optimisation process, in the simulation tests, the five-storey benchmark structure is subjected to four earthquake ground accelerations defined in the benchmark problems (El-Centro 1940, Hachinohe 1968, Kobe 1995 and Northridge 1994), among which El Centro and Hachinohe earthquakes represent far-field, moderate seismic events while Kobe and Northridge earthquakes are representative for near-field, more severe ground movements. All the excitations are applied with the full intensity for the evaluation of the proposed system's performance.

Among all types of responses, floor acceleration is one of the most significant ones to indicate the seismic-proof performance of the isolation system. For low- to mid-rise buildings, normally, the first mode is dominantly excited during an earthquake attack. Therefore, the floor acceleration increases with the height of the building. Hence, the time histories of the top floor accelerations of the five cases are plotted in Fig. 10. As can be seen in Fig. 10, all four isolation systems are capable of reducing the top floor acceleration in varying degrees. However, the optimised storey isolation system achieves the best performance in acceleration reduction. It is able to not only control the peak value of response when the major earthquake energy strikes, but also maintain the response to a rather low level on the whole time domain. As for the passive controlled isolation systems, no matter base isolation or storey isolation, the performance shows a great dependence on the type of earthquake excitation, especially for passive storey isolation system, which shows acceptable performance in El-Centro, Kobe and Hachinohe earthquakes but worse than the other three isolation systems in Northridge earthquake. Another noteworthy fact is that the performance of the passive storey isolation system shows lower frequency of those of the two base isolation systems, which indicates that the storey isolation system can endow the structure larger adjustable range of frequency so as to better avoid resonance of external excitations.

As mentioned in Introduction section, the most concerned issue of a base isolation system is the large demand in base displacement tolerance. The storey isolation system was proposed to distribute flexibility along the structure so as to effectively relieve the base displacement burden. To this end, the time history of the base displacement is adopted as another evaluation criteria of the isolation system. The base displacements of all five structures under four earthquakes are displayed in Fig. 11. It is obvious in Fig. 11 that the two passive controlled base isolation systems lead to larger base displacement than bare building under all four earthquakes As for passive storey isolation system, although it achieves smaller base displacement than fixed base buidling when subjected to Kobe earhtquake, it still results in increasing base displacement under three other earthquakes and the displacement is even larger than those base isolation system under

Hachinohe and Northridge earthquakes. Nevertheless, the optimised storey isolation system attains smaller base displacement than all the other three isolation systems under all four earhtquakes and the its base disolacement is even smaller than fixed base building under El-Centro, Kobe and Hachinohe earthquakes. Even under Northridge earthquake, the displacement of storey isolation system is just slightly larger than that of the bare building.

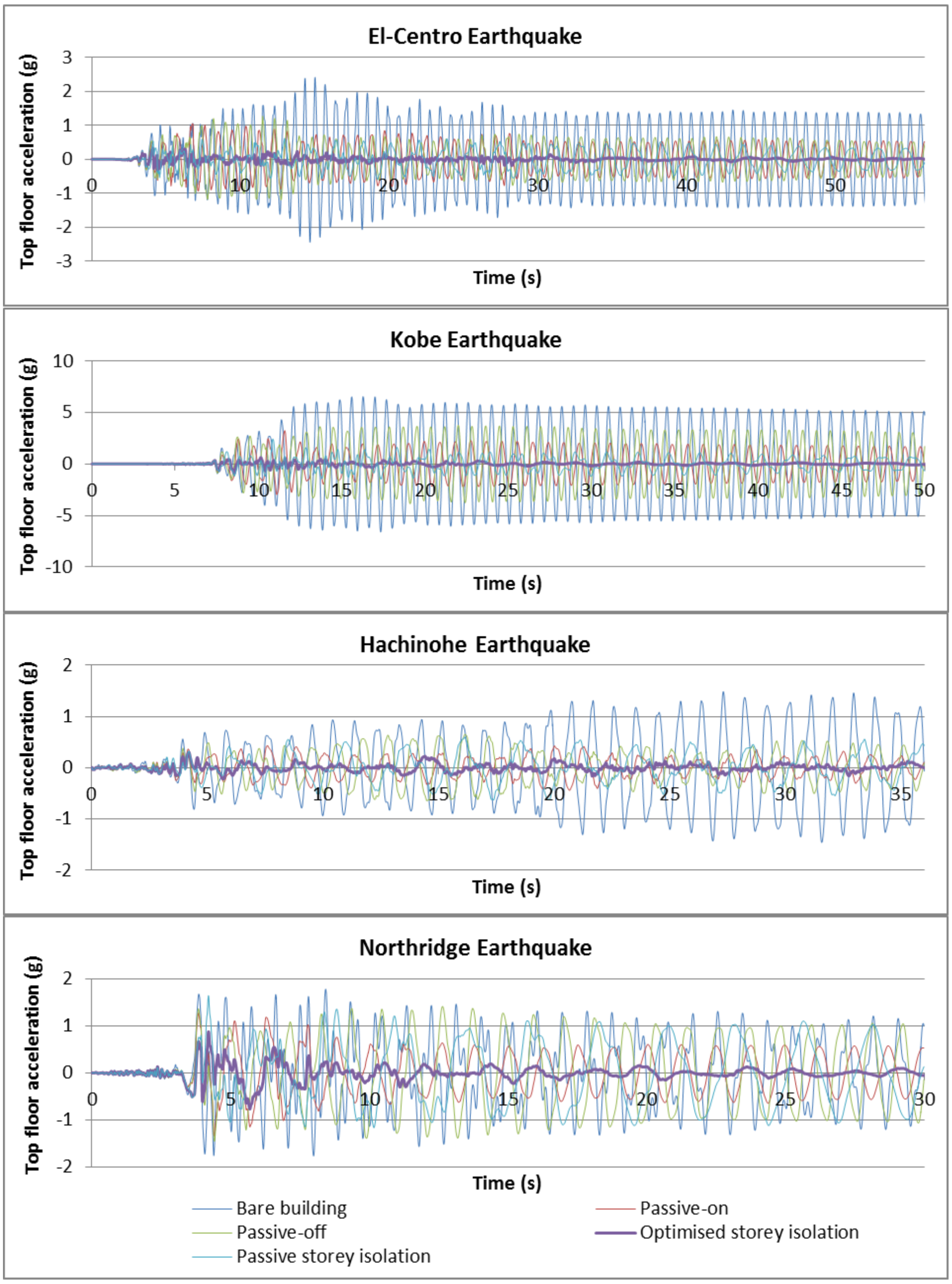

Fig. 10 Time history of top floor acceleration under four earthquakes

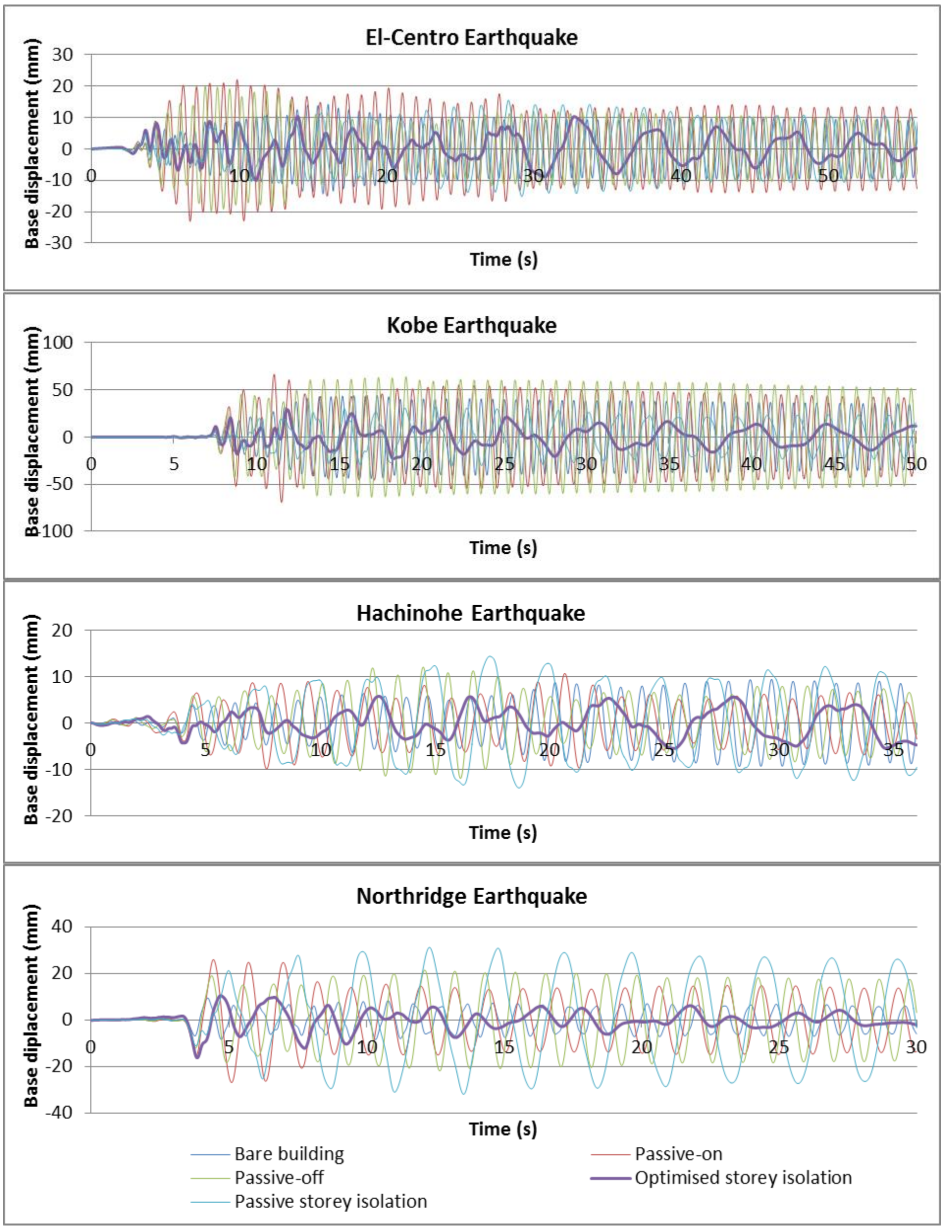

Fig. 11 Time history of base displacement under four earthquakes

Besides time histories of the top floor acceleration and base displacement, the peak acceleration and inter-storey drift are also of great interest. Meanwhile, the peak displacement versus floor height can also provide an approximate building profile when the movement is at greatest intensity. Therefore, Figs. 12, 13 and 14 illustrate the peak acceleration, relative displacement, inter-storey drift, respectively, versus floor height. It is clearly shown in Fig. 12 that the acceleration of the fixed base building increases with the floor number, which proves that the first mode is the principle mode excited. The optimised storey isolation system shows the greatest acceleration reduction and both base isolation systems can also effectively put down the acceleration at each floor. However, both passive controlled base isolation system and the passive storey isolation system show great reliance on the earthquake, which reveals the natural defect of the passive isolation system. As shown in Fig. 14, the relative displacement increases raises as the floor height develops. The optimised storey isolation system shows smallest base displacement in all four isolation mechanisms but the displacement exceeds the base isolation systems' as the level becomes higher. Such phenomenon makes sense in that the storey isolation system is much more flexible in the structure above ground while the base isolation system is only flexible at the base level. It is worth paying attention that the acceleration and displacement profiles of the base isolation systems are close to vertical lines under all earthquakes, which indicates that the movement of superstructure in these cases can be approximately regarded to a rigid body motion. The essence of the rigid body motion lies in effects of protecting structural elements of the superstructure.

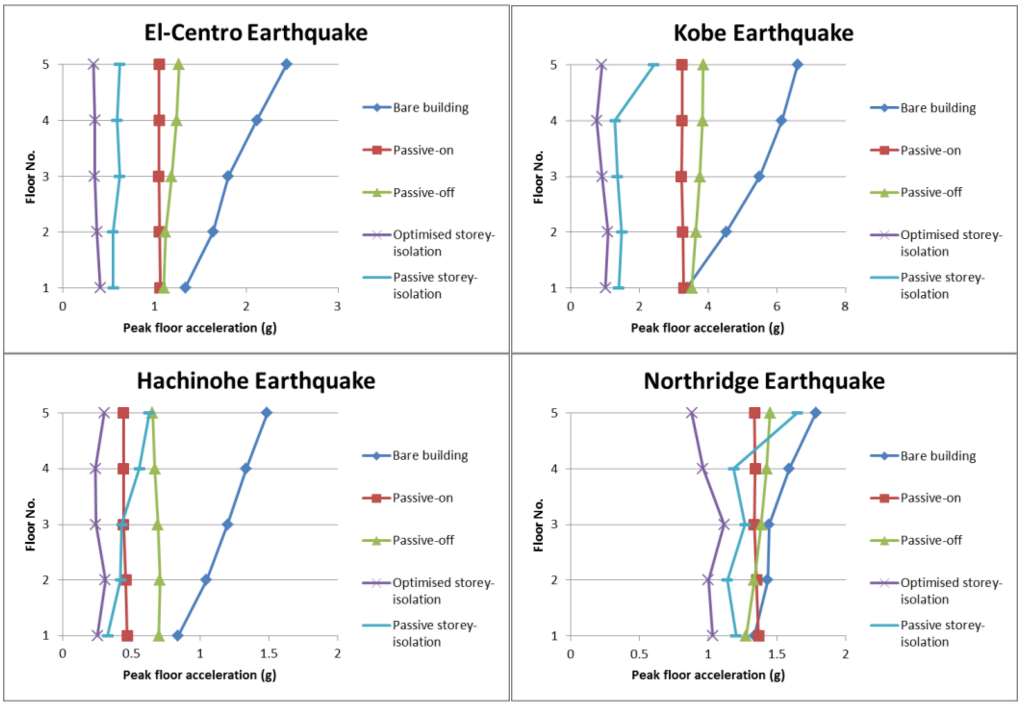

Fig. 12 Peak floor acceleration vs floor No.

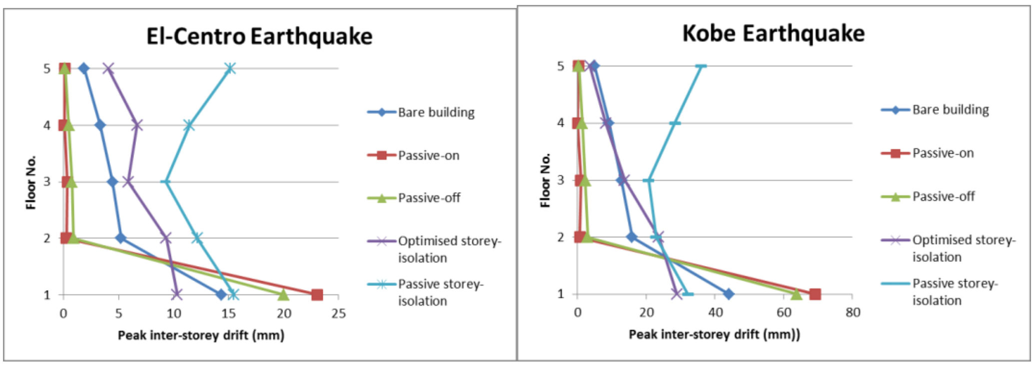

Fig. 13 Peak inter-storey drift vs floor No.

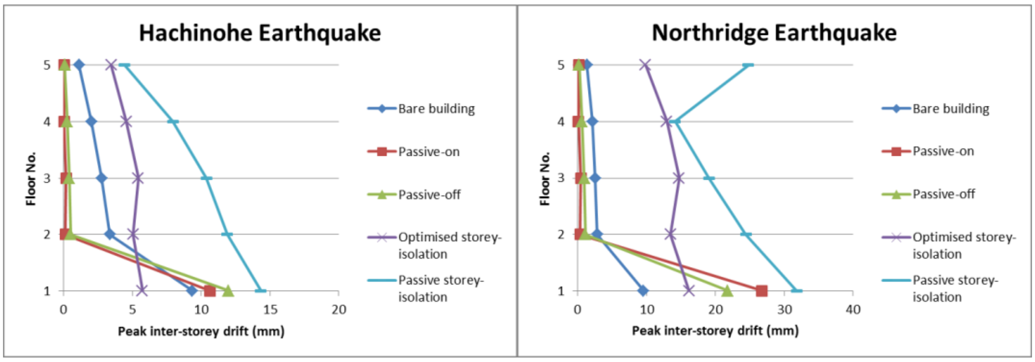

Fig. 13 Continued

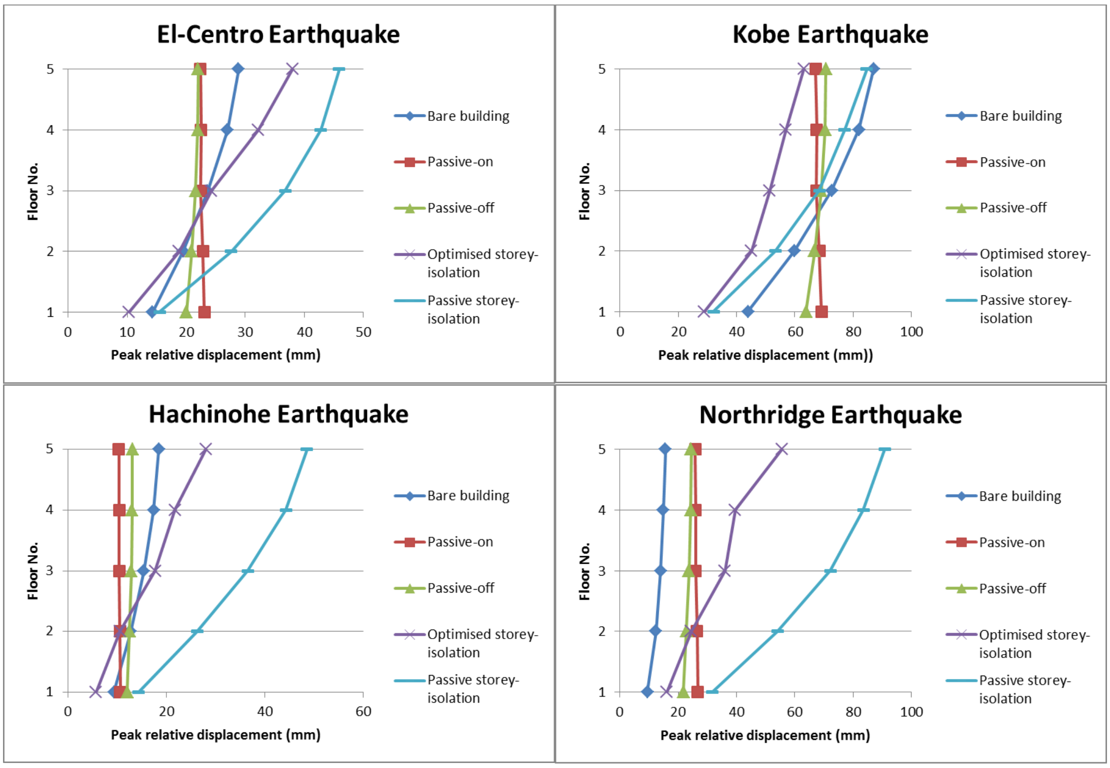

Fig. 14 Peak relative displacement vs floor No.

Peak inter-storey drift at each floor shown in Fig. 13 represents the relative movement between the adjacent floors, which implies the potential damage to the structural elements of the building. As displayed in Fig. 13, the base isolation systems show great potential in cutting down the inter-storey drift of the structure. The reason has been explained in last paragraph. Given that the floor height of the five-storey benchmark building is 600 mm, although the optimised storey isolation system didn't achieve as good inter-storey drift performance as base isolation systems, its inter-storey drift is still acceptable. Meanwhile, the fact that the optimised storey isolation system has better performance than the passive-on storey isolation system shows the potential of the adjustable storey isolation system to further decrease the inter-storey drift response with better control algorithms. Last but not least, the passive-on storey isolation system shows extreme large acceleration and inter-storey drift at some levels under certain earthquake, which can be attributed to the appearance of whipping effect. In contrast, the optimised storey isolation system doesn't suffer from such effect, meaning the smart MRE isolators' adjustable characteristics receive good influence when proper control method applied.

6. Conclusions

In this paper, an innovative storey isolation system utilising MRE isolators was proposed. The proposed isolation system aims to address the issue of excessive base displacement demand of a base isolation system by distributing the isolation efforts at strategic locations alongside the superstructure instead of concentrating it at the base level. Meanwhile, the storey isolation system is also able to cope with the situation where the structure has different seismic requirements at specific levels. The adjustable shear stiffness of the MRE isolators endows the storey isolation system large adaptability and controllability so as to better suppress the seismic responses of the protected structure. Meanwhile, the dynamic feature of MRE isolators can also be adjusted to cope with the parameter changes in the protected structure due to occurrence of damages. NSGA-II with DCD has been adopted to acquire optimisation of the storey isolation parameters. Comprehensive simulation studies have been conducted to compare the seismic protection performances of the bare building, passive-on controlled base-isolated building, passive-off controlled base-isolated building, passive-on controlled storey-isolated building and optimised storey-isolated building. Simulation results indicate that the optimised storey isolation system is capable of significantly mitigating the floor acceleration and base displacement. Moreover, it effectively resolved the whipping effect problem in passive controlled storey isolation systems.

Acknowledgements

This work was supported by Australian Research Council through Discovery Project (Grant No. DP150102636) as well as Blue Sky Research Fund from Faculty of Engineering and IT, University of Technology Sydney (UTS).

References

Chey, M.H., Chase, J.G., Mander, J.B. and Carr, A.J. (2009), "Semi-active control of mid-story isolation building system", *Proceeding of Asia Korean Conference on Advanced Science & Technology*.

Chey, M.H., Chase, J.G., Mander, J.B. and Carr, A.J. (2013), "Innovative seismic retrofitting strategy of added stories isolation system", *Front. Struct. Civ. Eng.*, **7**(1), 13-23.

Forcellini, Davide and James Marshall Kelly (2013), "Analysis of the large deformation stability of elastomeric bearings", *J. Eng. Mech*., ASCE, **140**(6), 04014036.

Gilmore, A.T. (2012), "Options for sustainable earthquake-resistant design of concrete and steel buildings", *Earthq. Struct.*, **3**(6), 783-804.

Gu, X., Li, J. and Li, Y. (2014), "Innovative semi-active storey isolation system utilising novel magneto-rheological elastomer base isolators", *Proceeding of 23rd Australasian Conference on the Mechanics of*

Structures and Materials (ACMSM23), Byron Bay, Australia, 9-12 December.
Jangid, R.S. and Datta, T.K. (1995), "Seismic behaviour of base-isolated buildings: A state-of-the art review", *P. I. Civ. Eng.-Struct. Build.*, **110**(2), 186-203.
Jangid, R.S. and Kelly, J.M. (2001), "Base isolation for near-fault motions", *Earthq. Eng. Struct. Dyn.*, **30**(5), 691-707.
Jin, J.M., Tan, P., Zhou, F.L., Ma, Y.H. and Shen, C.Y. (2012), "Shaking table test study on mid-story isolation structures", *Adv. Mater. Res.*, **446**, 378-381.
Johnson, E.A., Ramallo, J.C., Spencer Jr, B.F. and Sain, M.K. (1998), "Intelligent base isolation systems", *Proceedings of the Second World Conference on Structural Control*, USA, June.
Kawamura, S., Sugisaki, R., Ogura, K., Maezawa, S., Tanaka, S. and Yajima, A. (2000), "Seismic isolation retrofit in Japan", *12th World Conference on Earthquake Engineering*.
Kelly, J.M. (1981), "A seismic base isolation: its history and prospects", *Joint sealing and bearing system for concrete structures: world congress on joints and bearings*, IRN11891798, Published by American Concret Institute, 549-586.
Kelly, J.M. (1986), "Aseismic base isolation: review and bibliography", *Soil Dyn. Earthq. Eng.*, **5**(4), 202-216.
Kelly, J.M. (1993), "State-of-the-art and state-of-the-practice in base isolation", *Seminar on Seismic Isolation, Passive Energy Dissipation and Active Control (ATC-17-1)*, Applied Technology Council, Redwood City.
Li, Y., Li, J. and Li, W. (2013a), "Design and experimental testing of an adaptive magneto-rheological elastomer base isolator", *2013 IEEE/ASME International Conference on Advanced Intelligent Mechatronics*, Wollongong, Australia, July.
Li, Y., Li, J. and Samali, B. (2012), "A novel adaptive base isolator utilising magnetorheological elastomer", *22nd Australasian Conference on the Mechanics of Structures and Materials*, Sydney, Australia, December.
Li, Y., Li, J., Tian, T. and Li, W. (2013b), "A highly adjustable magneto-rheological elastomer base isolator for applications of real-time adaptive control", *Smart Mater. Struct.*, **22**(9), 095020.
Murakami, K., Kitamura, H., Ozaki, H. and Teramoto, T. (2000), "Design and analysis of a building with the middle-story isolation structural stystem", *12th World Conference of Earthquake Engineering*, **857**.
Pan, T.C., Ling, S.F. and Cui, W. (1993), "A new concept for reducing vibration of buildings under seismic loading", *Proceedings of Asia-Pacific Vibration Conference*, Kitakyshu, Japan.
Pan, Tso-Chien, Shih-Fu Ling and Wei Cui (1995), "Seismic response of segmental buildings", *Earthq. Eng. Struct. Dyn.*, **24**(7), 1039-1048.
Pan, Tso-Chien and Wei Cui (1998), "Response of segmental buildings to random seismic motions", *ISET J. Eng. Technol.*, **35**(4), 105-112.
Ryan, Keri L. and Curtis L. Earl (2010), "Analysis and design of inter-story isolation systems with nonlinear devices", *J. Earthq. Eng.*, **14**(7), 1044-1062.
Samali, B., Li, J., Mayol, E. and Wu, Y.M. (1999), "System identification of a five storey benchmark model using modal analysis", *Proceedings of the International Conference on Applications of Modal Analysis*, Gold Coast, Queensland, Australia.
Skinner, Robert Ivan, William H. Robinson and Graeme H. McVerry (1993), *An introduction to seismic isolation*, John Wiley & Sons.
Sueoka, Toshiyuki, Shingo Torii and Yasuhiro Tsuneki (2004), "The application of response control design using middle-story isolation system to high-rise building", *13th World Conference on Earthquake Engineering*, August.
Tasaka, M., Mori, N., Yamamoto, H., Murakami, K. and Sueoka, T. (2008), "Applying seismic isolation to buildings in Japan-retrofitting and middle-story isolation", *Proceeding of the 18th Analysis and Computation Specialty Conference, ASCE Structures Congress*, Vancouver, BC, Canada.
Tornello, M.E. and Sarrazin, M. (2012), "Base-isolated building with high-damping spring system subjected to near fault earthquakes", *Earthq. Struct.*, **3**(3-4), 315-340.

Torunbalci, N. and Ozpalanlar, G. (2008), "Earthquake response analysis of mid-story buildings isolated with various seismic isolation techniques", *The 14th World Conference on Earthquake Engineering*, Beijing, China.

Wang, F., Zhang, N. and Huang, Z. (2016), "Estimation of earthquake induced story hysteretic energy of multi-Story buildings", *Earthq. Struct.*, **11**(1), 165-178.

Wu, Y. and Samali, B. (2002), "Shake table testing of a base isolated model", *Eng. Struct.*, **24**(9) 1203-1215.

Xu, Z., Hu, M. and Zhou, F. (2004), "Discussion on mid-story isolation of building", *Earthq. Resist. Eng.*, **5**, 004.

Yu, Y., Li, Y. and Li, J. (2015), "Parameter identification and sensitivity analysis of an improved LuGre friction model for magnetorheological elastomer base isolator", *Meccanica*, **50**(11), 2691-2707.

Yu, Y., Li, Y., Li, J. and Gu, X. (2016), "A hysteresis model for dynamic behaviour of magnetorheological elastomer base isolator", *Smart Mater. Struct.*, **25**(5), 055029.

JL